# Supplementary Information to:

# Thermodynamics of amyloid-β fibril elongation: atomistic details of the transition state

Roberto A. Rodriguez[1], Liao Y. Chen[1], Germán Plascencia-Villa[1], George Perry[2]

[1]Department of Physics and Astronomy, University of Texas at San Antonio, San Antonio, TX 78249, USA

[2]Department of Biology and Neurosciences Institute, University of Texas at San Antonio, San Antonio, TX 78249, USA

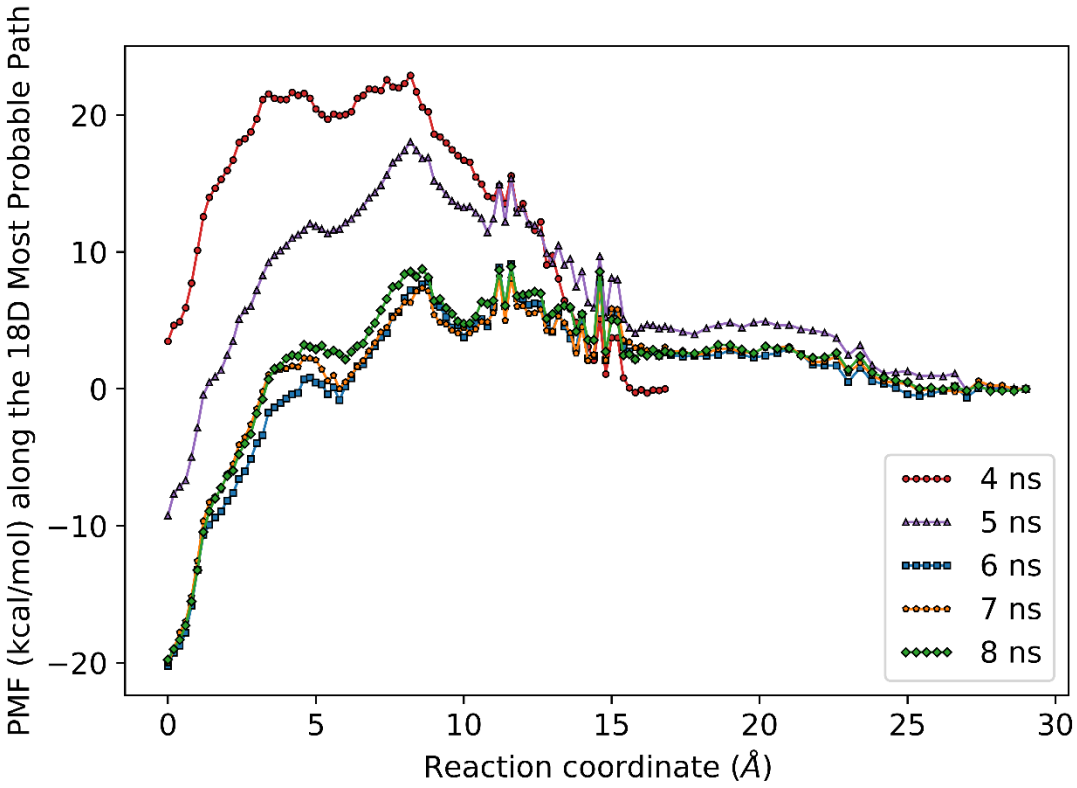


Figure S1: The effect of equilibration time on the convergence of the free energy profiles. The initial set (red circles) was equilibrated for 4 ns, after which we performed a 1 ns sampling simulation. The second set (purple triangles) was continued from the initial set, that is, the resulting state of the 4 + 1 ns total simulation time for the initial set was used to conduct another 1 ns sampling simulation. This was repeated for the subsequent sets (where each set was continued from the previous one) until the free energy profile converged. The last three sets (6, 7, and 8 ns) were those used for the results presented in the main text.

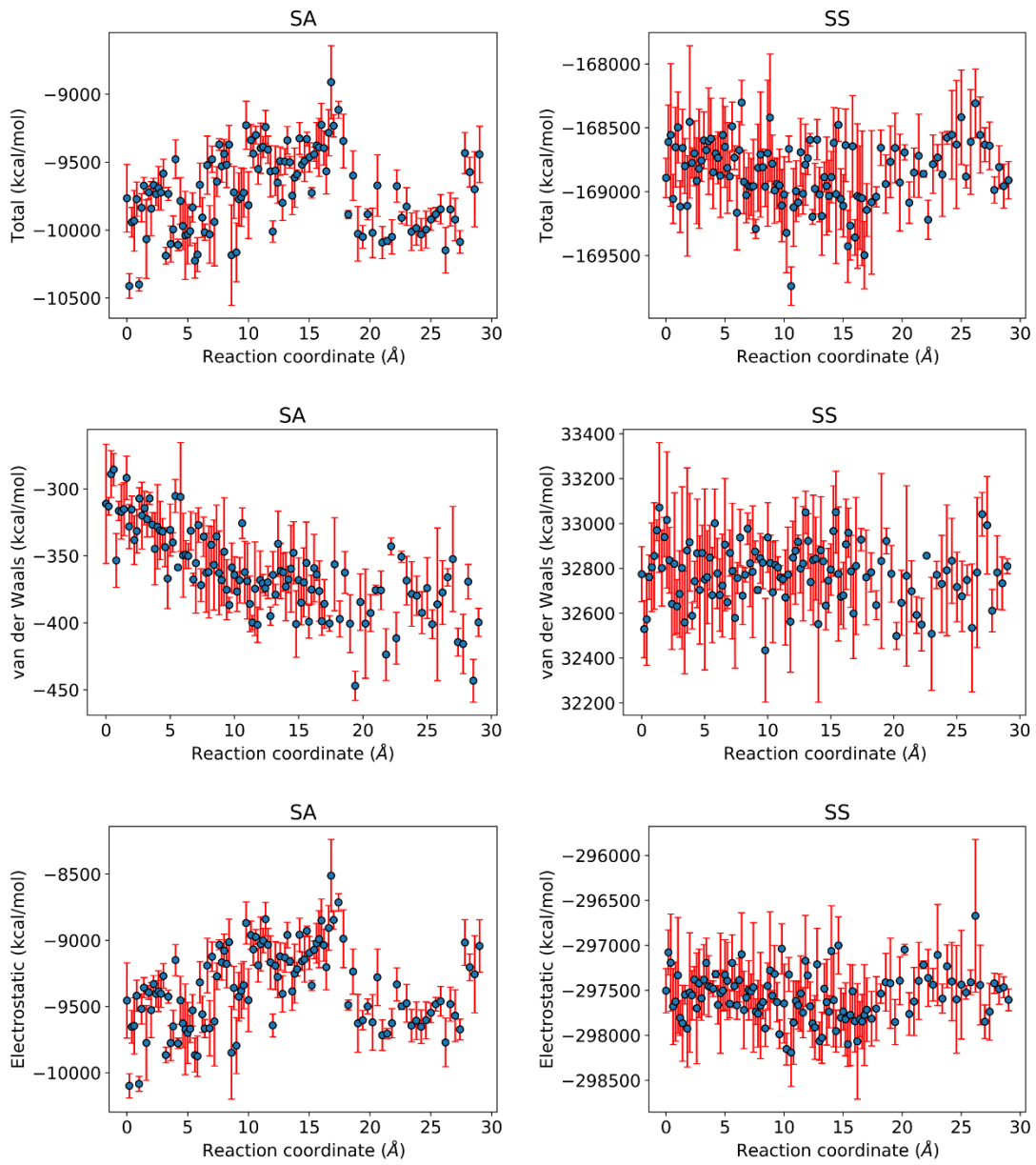


Figure S2: Energy (total, van der Waals, and electrostatic) of the solvent-aggregate (SA) and the solvent-solvent (SS) subsystems as a function of P0's displacement (see Figure 1 of the main text for the definition of P0).

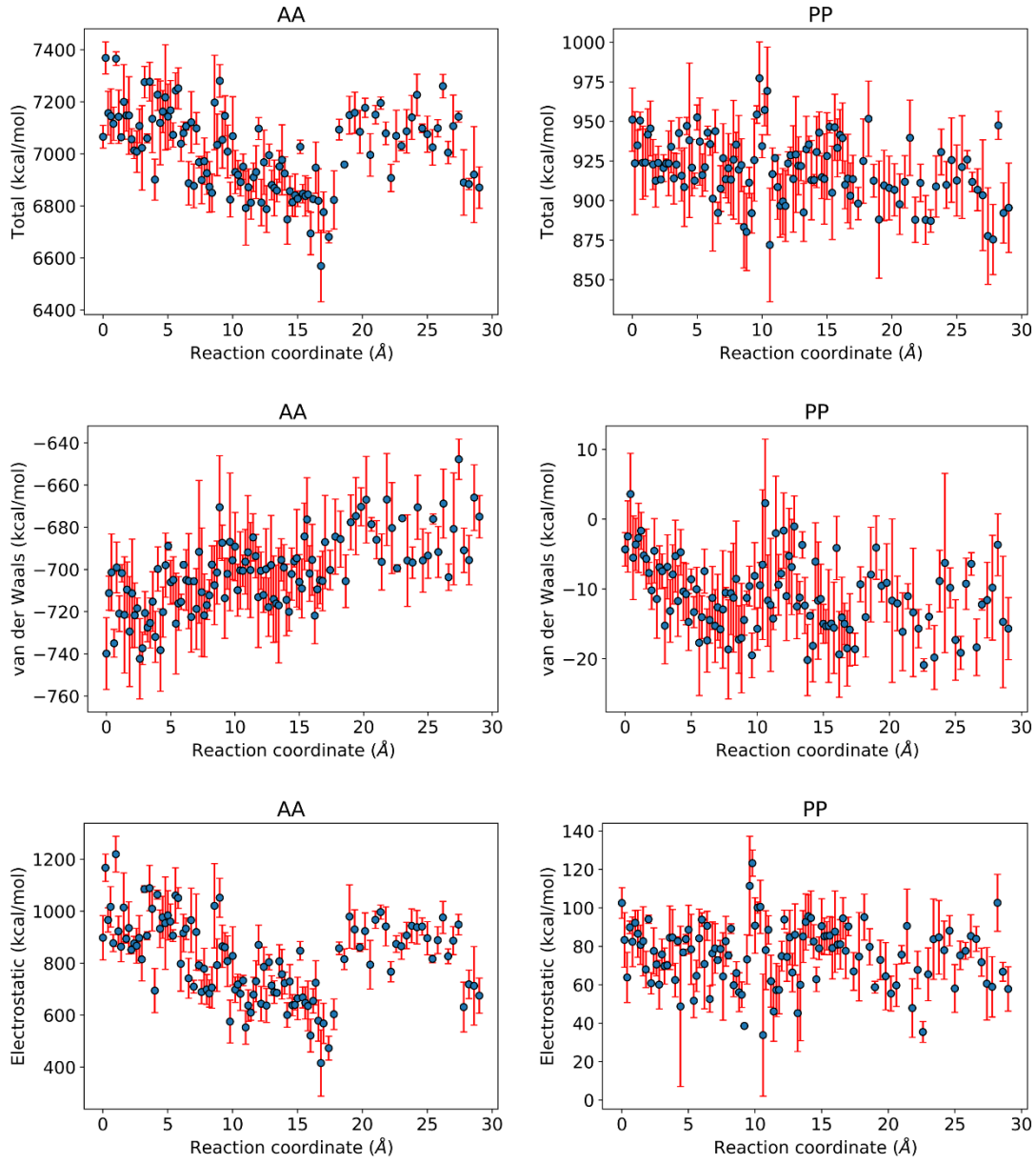


Figure S3: Energy (total, van der Waals, and electrostatic) of the aggregate-aggregate (AA) and the peptide-peptide (PP) subsystems as a function of P0's displacement.

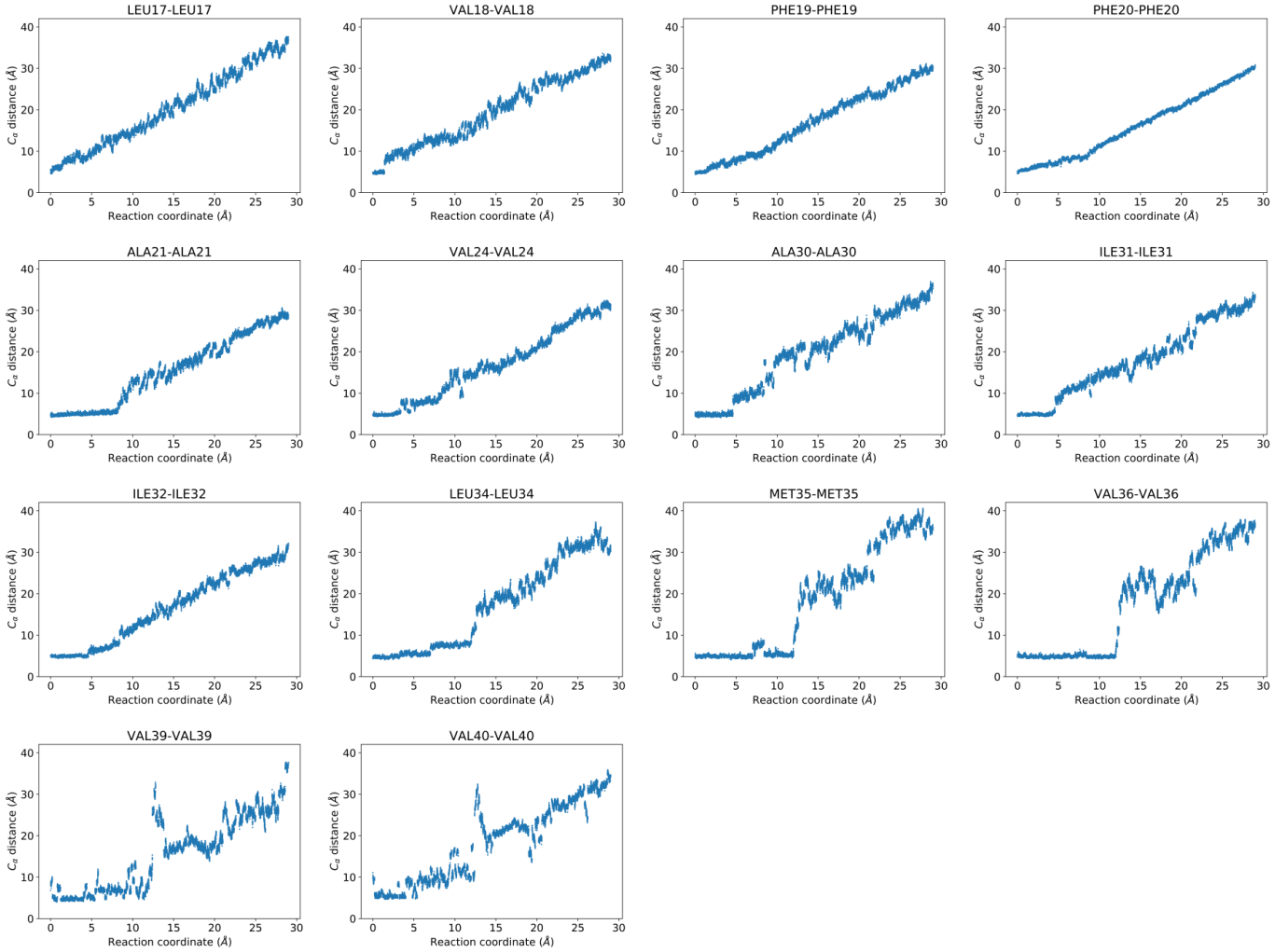


Figure S4: Distance between the alpha carbons of P0 and P1 (see Figure 2 of the main text) for every hydrophobic residue of the $A\beta_{15\text{-}40}$ Iowa mutant model as a function of the reaction coordinate.

# Computing the PMF

We now elaborate on our methodology to compute the free energy profile shown in Figure 1 of the main text. Let us consider the binding process of a "ligand" and a protein (the ligand in our case being the steered monomer and the protein being the filament core). By steering a selected number of atoms on a ligand we can decompose its Gibbs free energy of binding into an "energetic" (PMF) and an "entropic" contribution (see below for a qualification of these terms) as follows[1,2]:

$$\Delta G = \Delta W_{0,\infty} - k_B T \ln\left(c_0 Z_{n,0} / Z_{n,\infty}\right). \tag{1}$$

The PMF difference between the bound and the unbound states $\Delta W_{0,\infty}$ is given by

$$\Delta W_{0,\infty} = W\left(\mathbf{r}_{1,0},\ldots,\mathbf{r}_{n,0}\right) - W\left(\mathbf{r}_{1,\infty},\ldots,\mathbf{r}_{n,\infty}\right). \tag{2}$$

In Eqs. (1) and (2), $n$ represents the number of atoms chosen to steer, while the subscripts $0,\infty$ refer to the bound and unbound states, respectively. In Eq. (1), $k_B$ is the Boltzmann constant, $T$ is the absolute temperature, $c_0$ is the standard concentration (6.02), $Z_{n.0}$ is the partial partition function of the $n$ steered atoms in the bound state, and $Z_{n,\infty}$ is the partial partition function of the $n$ steered atoms in the unbound state. In Eq. (2), the position vectors $\left(\mathbf{r}_{1,0},\ldots,\mathbf{r}_{n,0}\right)$ of the $n$ steered atoms are the initial point in the $3n$-D space that represents the configuration of the ligand in the bound state. This point may be connected to the final point $\left(\mathbf{r}_{1,\infty},\ldots,\mathbf{r}_{n,\infty}\right)$ via an arbitrary curve, since the Gibbs free energy (and by extension the PMF) is a function of state (note that this *not* mean that different steering paths will exhibit the same barrier, if they exhibit one at all).

From basic thermodynamics, we have the following relationship between the Gibbs free energy $\Delta G$, the enthalpy $\Delta H$, the entropy $\Delta S$, and the absolute temperature $T$:

$$\Delta G = \Delta H - T\Delta S. \tag{3}$$

When the only quantity of interest is $\Delta G$, little interest needs to be paid into the feasibility of separating the Gibbs free energy into enthalpic and entropic contributions. Otherwise, special care needs to be taken when interpreting Eq. (1). The PMF $\Delta W_{0,\infty}$ doesn't correspond exactly to the enthalpy $\Delta H$, nor does the ratio of the partition functions exactly correspond the entropic term $T\Delta S$. This is because, in the

computation of the PMF, the $n$ steered centers are typically fixed along the steering path, precluding them from contributing to the entropic term. This contribution is precisely what is accounted for in the "entropic" term of Eq. (1). If the ligand has $N$ total atoms, $n$ of which are steered and fixed along the steering path (and thus $N-n$ atoms are freely subject to the stochastic dynamics of the system), then the PMF may be schematically decomposed as

$$\Delta W_{0,\infty} = \Delta H - T\Delta S\left(N-n\right), \tag{4}$$

where $\Delta S\left(N-n\right)$ represents the entropic contributions of the $N-n$ atoms which are free to fluctuate. Thus, if this term is small enough, the computed PMF difference will be close to the enthalpy change.

The $3n$-D PMF $W\left(\mathbf{r}_1,\ldots,\mathbf{r}_n\right)$ as a function of the phase space coordinate $\left(\mathbf{r}_1,\ldots,\mathbf{r}_n\right)$ may be computed in multiple ways. In this work, we used thermodynamic integration as applied to $n$ steered atoms[3]. We divided the path between the bound and unbound states into discrete states, indexed by a generalized parameter $\lambda$. The initial and final states are then connected via a curve in the $3n$-D space denoted as

$$\mathbf{u}\left(\lambda\right) = \left(\mathbf{r}_1\left(\lambda\right),\ldots,\mathbf{r}_n\left(\lambda\right)\right), \tag{5}$$

where $\mathbf{u}\left(\lambda=0\right) = \left(\mathbf{r}_{1,0},\ldots,\mathbf{r}_{n,0}\right)$ is the initial state and $\mathbf{u}\left(\lambda=1\right) = \left(\mathbf{r}_{1,\infty},\ldots,\mathbf{r}_{n,\infty}\right)$ is the final state. We then have[3]

$$\Delta W_{0,\infty} = \int_{\lambda=0}^{\lambda=1} \mathrm{d}\mathbf{u}\left(\lambda\right)\cdot\left\langle -\frac{\partial H}{\partial \mathbf{u}}\right\rangle_{\mathbf{u}\left(\lambda\right)}, \tag{6}$$

where $H$ is the Hamiltonian of the entire system. The term inside the angular brackets is the $3n$-D gradient of the Hamiltonian with respect to the positions of the $n$ steered atoms, which is nothing other than the force acting on the steered atoms by the rest of the system. The angular brackets represent that. at each discrete state $\mathbf{u}\left(\lambda\right)$, we compute the mean force acting on the steered atoms. This returns a $3n$-D force vector, which is multiplied (dot product) with the $3n$-D vector containing the displacements along the path. In the case of the present work, we chose as the initial state the crystal structure by Sgourakis et al.[4] The steering path was chosen along the fibril axis, and six alpha carbons (those of residues 15, 20, 25, 27, 33, and 40) were steered, disallowing any fluctuations along the path.

An accurate estimate of the Arrhenius barrier $\Delta H^{\ddagger}$ (the difference in enthalpy between the transition state and the unbound state) is a different matter. This is dependent on the steering path chosen to separate

the bound and unbound states. In addition, different choices of steering atoms may increase the entropic term in Eq. (4), leading to a poorer estimate of $\Delta H^{\ddagger}$. In our specific case, by fixing alpha carbons more or less uniformly distributed along the beta hairpin structure of the monomer, we are able to severely constrain the conformation of the $N$ free atoms on the peptide. Therefore, the conformational fluctuations (and by extension the entropy) at the transition state will be very similar to the same in the unbound state, making the estimate of $\Delta H^{\ddagger}$ based on the PMF more accurate. This can also be noted by considering the well-known entropy-enthalpy compensation observed in amyloid growth measurements. The positive value for the activation entropy $\Delta S^{\ddagger}$ is due to the limited space the monomer can sample at the unbound state (due to, e.g., burying its hydrophobic core) whereas the conformational changes at the transition state are much larger, since the monomer isn't uniformly surrounded by water anymore and can engage in stabilizing hydrophobic contacts with the topmost layer of the filament. Therefore, our strategy of restricting the conformation of the monomer along the steering pathway makes it so the relative fluctuations at the transition state and the unbound state are of similar magnitude and thus cancel, leaving behind a PMF difference between the transition and unbound states that is almost completely enthalpic.

The path chosen to steer the monomer is another factor that can affect the results. Our choice of steering along the fibril axis is guided by our concern for steric clashes when performing the mean force sampling at the discrete states $\mathbf{u}(\lambda)$ as dictated by Eq. (6). Since the system is equilibrated at each state before the force sampling takes place, we propose that the path taken by the steered peptide is close to the "most probable path", since the degrees of freedom orthogonal to the steered atoms are allowed to relax according to the stochastic dynamics. A steering path at an angle to the fibril axis increases the "contact time" between the steered monomer and the filament core, as well as increasing steric clashes between them, which in turn can unphysically increase the Arrhenius barrier. This can be understood by noting that, since the PMF is a function of state, the initial and final states of a *converged* profile must remain invariant with respect to the steering angle. Unphysical steric clashes, which would increase the energy at each discrete state, would result in an unphysically large barrier.

# References

(1) Chen, L. Y. (2015) Hybrid Steered Molecular Dynamics Approach to Computing Absolute Binding Free Energy of Ligand–Protein Complexes: A Brute Force Approach That Is Fast and Accurate. *J. Chem. Theory Comput. 11*, 1928–1938.

(2) Rodriguez, R. A., Yu, L., and Chen, L. Y. (2015) Computing Protein–Protein Association Affinity with Hybrid Steered Molecular Dynamics. *J. Chem. Theory Comput. 11*, 4427–4438.

(3) Chen, L. Y. (2017) Thermodynamic Integration in 3n Dimensions without Biases or Alchemy for Protein Interactions. *bioRxiv* 150870.

(4) Sgourakis, N. G., Yau, W.-M., and Qiang, W. (2015) Modeling an In-Register, Parallel "Iowa" Aβ Fibril Structure Using Solid-State NMR Data from Labeled Samples with Rosetta. *Structure 23*, 216–227.

(5) Young, L. J., Schierle, G. S. K., and Kaminski, C. F. (2017) Imaging Aβ(1–42) fibril elongation reveals strongly polarised growth and growth incompetent states. *Phys. Chem. Chem. Phys. 19*, 27987–27996.